PHYSICAL REVIEW E **81**, 025205(R) (2010)

Controlling synchrony by delay coupling in networks: From in-phase to splay and cluster states

Chol-Ung Choe,[1,2] Thomas Dahms,[1] Philipp Hövel,[1] and Eckehard Schöll[1,*]
[1]*Institut für Theoretische Physik, Technische Universität Berlin, 10623 Berlin, Germany*
[2]*Department of Physics, University of Science, Unjong-District, Pyongyang, Democratic People's Republic Korea*
(Received 8 August 2009; revised manuscript received 15 December 2009; published 25 February 2010)

We study synchronization in delay-coupled oscillator networks using a master stability function approach. Within a generic model of Stuart-Landau oscillators (normal form of supercritical or subcritical Hopf bifurcation), we derive analytical stability conditions and demonstrate that by tuning the coupling phase one can easily control the stability of synchronous periodic states. We propose the coupling phase as a crucial control parameter to switch between in-phase synchronization or desynchronization for general network topologies or between in-phase, cluster, or splay states in unidirectional rings. Our results are robust even for slightly nonidentical elements of the network.

DOI: 10.1103/PhysRevE.81.025205 PACS number(s): 05.45.Xt, 02.30.Ks, 05.45.Gg, 89.75.−k

Over the last decade, control of dynamical systems and stabilization of unstable states have become a central issue in nonlinear science [1]. In parallel, the study of coupled systems ranging from a few elements to large networks has evolved into a rapidly expanding field [2]. To determine the stability of synchronized oscillations in networks, Pecora and Carroll introduced a technique called *master stability function* (MSF) [3], which allows one to separate the local dynamics of the individual nodes from the network topology. Although some recent approaches have tried to extend this theory in the presence of time delays [4,5], up to now control and design of dynamic behavior in complex networks with time delay is still in its infancy.

In this Rapid Communication, we aim to fill this gap by developing analytical tools for a large class of delay-coupled networks and deriving analytical conditions for controlling the different states of synchrony. We identify the coupling phase as a crucial control parameter and demonstrate that by adjusting this phase one can deliberately switch between different synchronous oscillatory states of the network. We use a generic model describing a wide range of systems near a Hopf bifurcation, which allows for an analytical treatment, including the calculation of the Floquet exponents. These results promise broad applicability since the presence of time delays is of crucial importance in a variety of physical, biological, technological, social, ecological, or economic networks where they occur, e.g., as propagation delays in communication networks and laser arrays [6–8], electronic circuits [9], neural systems [10–12] or coupled Kuramoto phase oscillators [13–15], or in time-delayed feedback control loops [16].

We consider N-dimensional networks of delay-coupled Stuart-Landau oscillators ($j=1,\ldots,N$)

$$\dot{z}_j = f(z_j) + \sigma \sum_{n=1}^{N} a_{jn}[z_n(t-\tau) - z_j(t)], \tag{1}$$

with $z_j = r_j e^{i\varphi_j} \in \mathbb{C}$, time delay τ, and complex coupling strength $\sigma = Ke^{i\beta}$. Such phase-dependent couplings have been shown to be important in overcoming the odd-number limitation of time-delayed feedback control [17] and in anticipating chaos synchronization [18]. The topology of the network is determined by the real-valued adjacency matrix $\mathbf{A}=(a_{jn})$. Nonzero diagonal elements, for instance, correspond to networks with delayed self-feedback. In the following, we consider only constant row sum $\mu = \Sigma_n a_{jn}$ such that each node is subject to the same input for complete synchronization. This generalizes the common assumption of zero row sum in the MSF approach. The local dynamics of each element is given by the normal form of a supercritical (−) or subcritical (+) Hopf bifurcation:

$$f(z_j) = [\lambda + i\omega \mp (1 + i\gamma)|z_j|^2]z_j, \tag{2}$$

with real constants λ, $\omega \neq 0$, and γ. This system arises naturally as a generic expansion near a Hopf bifurcation, and is therefore often used as a paradigm for oscillators.

In the following, we focus on synchronous in-phase, cluster, and splay states with a common amplitude $r_j \equiv r_{0,m}$ and phases given by $\varphi_j = \Omega_m t + j\Delta\phi_m$ with $\Delta\phi_m = 2\pi m/N$. The integer m determines the specific state: in-phase oscillations correspond to $m=0$, while cluster and splay states correspond to $m=1,\ldots,N-1$. The cluster number d_c, which determines how many clusters of oscillators exist, is given by the least common multiple of m and N divided by m. $d_c=N$ corresponds to a splay state [19]. Using the abbreviation $\Phi_{n,m} = \beta - \Omega_m\tau + (n-j)\Delta\phi_m$, which is independent of j for in-phase oscillation in general networks and for splay and cluster states in ring configurations [20], we obtain

$$r_{0,m}^2 = \pm\left(\lambda - \mu K\cos\beta + K\sum_{n=1}^{N} a_{jn}\cos\Phi_{n,m}\right), \tag{3a}$$

$$\Omega_m = \omega \mp \gamma r_{0,m}^2 - \mu K\sin\beta + K\sum_{n=1}^{N} a_{jn}\sin\Phi_{n,m} \tag{3b}$$

as invariant solutions of $r_{0,m}$ and φ_j. The following discussion focuses on the supercritical case (upper signs), but a similar argument holds also for the subcritical Hopf normal form (see discussion at the end of this Rapid Communication).

*schoell@physik.tu-berlin.de

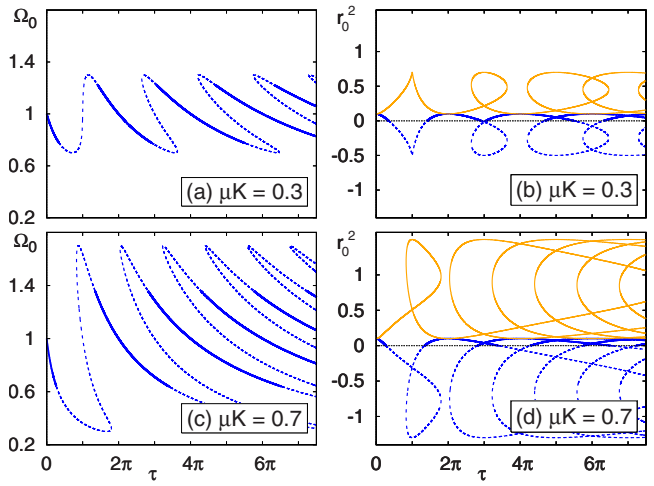

FIG. 1. (Color online) Collective frequency Ω_0 (left) and squared amplitude r_0^2 (right) of in-phase oscillation ($m=0$) vs time delay τ for different amplitude of the feedback strength [$\mu K=0.3$ and 0.7 in (a), (b) and (c), (d), respectively]. Black (blue) and gray (yellow) curves correspond to a feedback phase $\beta=0$ and $\beta=\Omega_0\tau$, respectively. Unphysical solutions ($r_0^2<0$) are dashed. For $\beta=\Omega_0\tau$ the curves in (a) and (c) have the same shape, but no unphysical solutions occur. Parameters: $\lambda=0.1$, $\omega=1$, and $\gamma=0$.

Figure 1 shows solutions of $r_0^2(r_0\equiv r_{0,0})$ and Ω_0 for in-phase oscillations ($m=0$) according to Eqs. (3) in dependence on the time delay τ for fixed feedback strength $\mu K=0.3$ and 0.7 in panels (a) and (b) and (c) and (d), respectively. The black (blue) lines show the behavior for the coupling phase $\beta=0$. The collective frequency Ω_0 is distributed around the intrinsic frequency $\omega=1$, where multiple solutions are obtained with increasing time delay τ. This behavior becomes more pronounced for higher μK (c). The collective amplitude also shows multivalued behavior; spurious solutions with $r_0^2<0$, which correspond to amplitude death, are indicated as dashed curves. For a coupling phase $\beta=\Omega_0\tau$, these unphysical solutions do not occur since $r_0^2\geq\lambda=0.1$ as shown by the gray (yellow) curves in (b) and (d). Note that for $\beta=\Omega_0\tau$ the shape of the Ω_0 curve in (a) and (c) is unchanged, but now *all* points are valid solutions.

Considering small deviations δr_j and $\delta\varphi_j$, i.e., $r_j=r_{0,m}(1+\delta r_j)$, $\varphi_j=\Omega_m t+j\Delta\phi_m+\delta\varphi_j$, $\xi_j=(\delta r_j,\delta\varphi_j)^T$, yields a variational equation for the synchronized state

$$\dot{\xi}=\mathbf{I}_N\otimes(\mathbf{J}_{0,m}^{\mp}-K\mathbf{\Psi}_m)\xi+K(\mathbf{A}\otimes\mathbf{R}_{n,m})\xi(t-\tau), \qquad (4)$$

with the $2N$-dimensional vector $\xi=(\xi_1,\ldots,\xi_N)^T$, the $N\times N$ identity matrix $\mathbf{I}_N$, and matrices $\mathbf{\Psi}_m=\begin{pmatrix}\Sigma_n a_{jn}\cos\Phi_{n,m} & -\Sigma_n a_{jn}\sin\Phi_{n,m}\\ \Sigma_n a_{jn}\sin\Phi_{n,m} & \Sigma_n a_{jn}\cos\Phi_{n,m}\end{pmatrix}$, $\mathbf{R}_{n,m}=\begin{pmatrix}\cos\Phi_{n,m} & -\sin\Phi_{n,m}\\ \sin\Phi_{n,m} & \cos\Phi_{n,m}\end{pmatrix}$, and $\mathbf{J}_{0,m}^{\mp}=\begin{pmatrix}\mp 2r_{0,m}^2 & 0\\ \mp 2\gamma r_{0,m}^2 & 0\end{pmatrix}$, which is an important generalization of the usual MSF approach.

In order to derive an analytical expression for stability, Eq. (4) has to be diagonalized in terms of $\mathbf{A}$. To succeed, the rotational matrix $\mathbf{R}_{n,m}$ must not depend on n. This is achieved in two cases: (i) by considering only in-phase synchronization ($m=0$) or (ii) by considering special network configurations.

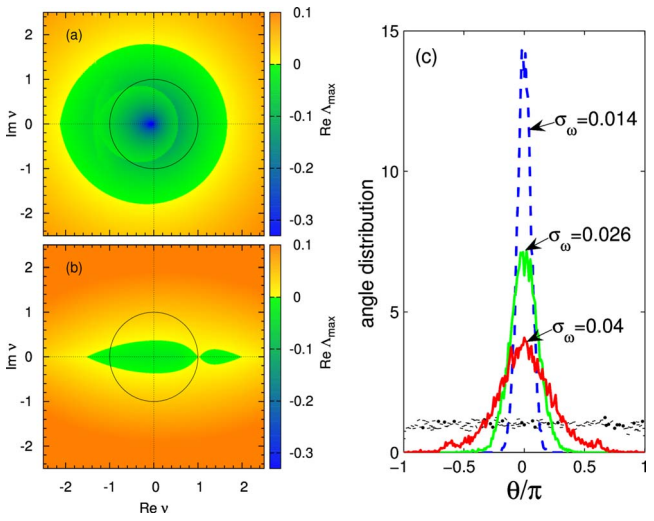

FIG. 2. (Color online) [(a) and (b)] Master stability function in the (Re ν,Im ν)-plane for $m=0$, $\beta=0$. The grayscale (color code) corresponds to the largest real part of the Floquet exponents for a given value of the product $K\nu$. All eigenvalues of the coupling matrix $\mathbf{A}$ for a unidirectional ring lie on the black circle. Parameters (a) $K\mu=0.3$, $\tau=2\pi$, (b) $K\mu=0.08$, $\tau=0.52\pi$, others as in Fig. 1. (c) Distribution of relative phases $\theta=\varphi_i-\Theta$ around the order parameter for 200 slightly nonidentical elements with different standard deviations σ_ω of the frequencies ω for $\beta=\Omega_0\tau$. Dotted (black) curve: $\beta=\Omega_0\tau+\pi$ (desynchronization). Other parameters as in (b).

In case (i), the matrix $\mathbf{R}_{n,0}=\mathbf{R}$ with $\Phi_{n,0}=\Phi_0$ does not depend on n and with $J_{0,0}^{\mp}\equiv J_0^{\mp}$ Eq. (4) simplifies to

$$\dot{\xi}=\mathbf{I}_N\otimes(\mathbf{J}_0^{\mp}-\mu K\mathbf{R})\xi+K(\mathbf{A}\otimes\mathbf{R})\xi(t-\tau). \qquad (5)$$

Diagonalizing $\mathbf{A}$, we arrive at the block-diagonalized variational equation:

$$\dot{\zeta}_k(t)=\mathbf{J}_0^{\mp}\zeta_k(t)-K\mathbf{R}[\mu\zeta_k(t)-\nu_k\zeta_k(t-\tau)], \qquad (6)$$

where ν_k is an eigenvalue of $\mathbf{A}$, $k=0,1,2,\ldots,N-1$, and $\nu_0=\mu$ corresponds to the dynamics in the synchronization manifold. Since the coefficient matrices in Eq. (6) do not depend on time, the Floquet exponents of the synchronized periodic state are given by the eigenvalues Λ of the characteristic equation

$$\det\{\mathbf{J}_0^{\mp}-\Lambda\mathbf{I_2}+K(-\mu+\nu_k e^{-\Lambda\tau})\mathbf{R}\}=0. \qquad (7)$$

Figures 2(a) and 2(b) depict the MSF, i.e., the largest real part of the Floquet exponents, calculated from Eq. (7) for different coupling parameters. Note that for a unidirectionally coupled ring all eigenvalues, i.e., $\nu_k=\exp(2\pi ik/N)$ with $k=0,1,\ldots,N-1$, are located on the black circle. Hence, for the choice of parameters in panel (a) all eigenvalues lie in the region of negative maximum real part of the Floquet exponent (stable in-phase solution), whereas the parameters in panel (b) do not allow for synchronization of the unidirectional ring. Furthermore, it can be shown using Gerschgörin's disk theorem [13] that the eigenvalues are located on or inside this circle $S(0,\mu)$ centered at zero with radius μ for any network topology without self-feedback (diagonal elements $a_{jj}=0$). The same holds for the circle $S(a_{jj},\mu)$ cen-

tered at a_{jj} if self-feedback (constant a_{jj}, $j=1\ldots,N$) is added while keeping the constant row sum condition. Note that the MSF is symmetric with respect to a change in sign of $\mathrm{Im}(\nu)$.

For coupling phases $\beta=\Omega_0\tau+2l\pi$ with integer l, i.e., $\Phi_0=2l\pi$, the characteristic equation (7) for the Floquet exponents Λ factorizes:

$$0=(K\nu_k e^{-\Lambda\tau}-K\mu\mp 2r_0^2-\Lambda)(K\nu_k e^{-\Lambda\tau}-K\mu-\Lambda). \quad (8)$$

In the supercritical case (upper sign), the dominant Floquet exponent is determined by the second factor in Eq. (8) which gives $\mathrm{Re}\,\Lambda<0$ for $K>0$ for any eigenvalue ν_k on or inside $S(0,\mu)$, taking into account $r_0^2>0$, and hence stable in-phase synchronization for any network topology without or with self-feedback, observing the constant row sum conditions. A similar equation arises for $\beta=\Omega_0\tau+(2l+1)\pi$ with Ω_0 obtained from Eq. (3b), and it can be shown by analogous arguments that there exist exponents Λ with positive real part, which results in desynchronization. In conclusion, the synchronous (in-phase) dynamics can be stabilized or destabilized by proper choice of the coupling phase β. These results are robust even if slightly nonindentical elements are considered. Figure 2(c) shows numerical simulations for all-to-all coupling of 200 elements with Gaussian frequency distributions around $\omega=1$ with different standard deviations σ_ω. Initial phases are chosen randomly as $\varphi_i\in[0,2\pi)$, and initial radii $r_i=\lambda$, $i=1,\ldots,N$. For $\beta=\Omega_0\tau$ the relative phases of the individual oscillators around the order parameter $Re^{i\Theta}\equiv\frac{1}{N}\sum_j\frac{z_j}{|z_j|}$ (in rotating coordinates) are distributed around a maximum (in-phase) with different sharpness according to σ_ω, whereas for $\beta=\Omega_0\tau+\pi$ the phase is uniformly distributed regardless of σ_ω (desynchronization).

We now consider case (ii), i.e., special network configurations, and exemplarily choose a unidirectional ring with $a_{i,i+1}=a_{N,1}=1=\mu$ and all other $a_{i,j}=0$. Then the matrix $\mathbf{R}_{n,m}=\mathbf{R}_m$ with $\Phi_{n,m}=\Phi_m=\beta-\Omega_m\tau+\Delta\phi_m$ does not depend on n and the diagonalization of Eq. (4) yields the same form as Eq. (6) with $\mu=1$, and $\mathbf{R}$ replaced by $\mathbf{R}_m$. The eigenvalues of $\mathbf{A}$ are explicitly given by $\nu_k=e^{2ik\pi/N}$, $k=0,1,\ldots,N-1$, and the Floquet exponents Λ can be calculated from the corresponding characteristic equation (7).

Figure 3(a) shows the stability boundaries of different dynamical scenarios in the (K,τ) plane for unidirectional coupling of $N=4$ oscillators. The coupling phase is fixed at $\beta=0$. The grayscale (color code) indicates regions of different multistability of in-phase ($m=0$), two-cluster ($m=2$), and splay states ($m=1$, $m=3$): black (blue), dark gray (red), light gray (green), and yellow (white) color corresponds to regions where one, two, three, or four of these dynamical states are stable, respectively.

Let us now consider the effects of the coupling phase β. The specific choice of $\beta=\Omega_0\tau$, $\Omega_1\tau-\pi/2$, $\Omega_2\tau-\pi$, and $\Omega_3\tau-3\pi/2$ enlarges the stability regime of the in-phase, splay ($m=1$), cluster, and splay ($m=3$) states, respectively, to the complete (K,τ) plane. This can be understood as follows. For $\Phi_m=2l\pi$, i.e., $\beta=\Omega_m\tau-\Delta\phi_m+2l\pi$ with integer l, the characteristic equation can again be factorized as Eq. (8). For the supercritical case, taking into account $r_0^2>0$ at $\beta=\Omega_m\tau-\Delta\phi_m+2l\pi$, it follows again that the dominant Floquet exponents have negative real part for any $K>0$ and τ. Therefore the unidirectional ring configuration of Stuart-Landau oscillators exhibits in-phase synchrony, splay states, and clustering according to the choice of the control parameter $\beta=\Omega_0\tau$, $\Omega_1\tau-2\pi/N$, or $\Omega_m\tau-2\pi m/N$ ($m>1$, $N>2$), respectively, for any values of the coupling strength and time delay.

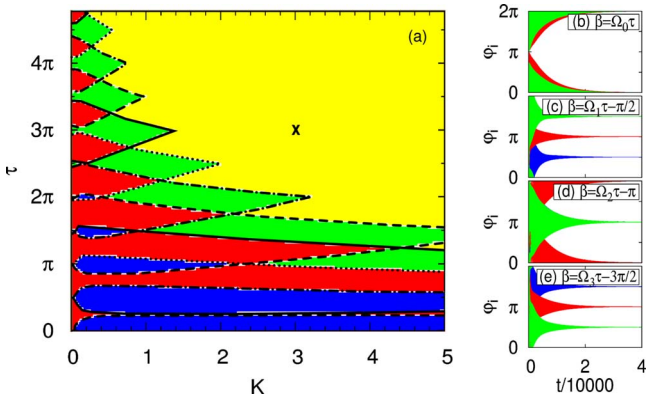

FIG. 3. (Color online) (a) Stability diagram of a unidirectional ring of $N=4$ oscillators in the (K,τ)-plane ($\beta=0$). Solid, dash-dotted, dashed, and dotted boundaries correspond to a stability change in in-phase ($m=0$), two-cluster ($m=2$), splay states with $m=1$, and $m=3$, respectively. The black (blue), dark gray (red), light gray (green), and white (yellow) regions denote multistability of one, two, three, and four of the above states. [(b)–(e)] Time series of the phase differences for a unidirectional ring of four slightly nonidentical oscillators: (b) $\beta=\Omega_0\tau$, (c) $\Omega_1\tau-\pi/2$, (d) $\Omega_2\tau-\pi$, (e) $\Omega_3\tau-3\pi/2$, with $\Omega_0=1$, $\Omega_1=0.839\,03$, $\Omega_2=1$, and $\Omega_3=1.160\,97$. Black (blue), dark gray (red), and light gray (green) lines denote the differences $\varphi_2-\varphi_1$, $\varphi_3-\varphi_1$, and $\varphi_4-\varphi_1$, respectively [in (b) and (d) black (blue) is hidden behind light gray (green)]. Parameters: $\lambda=0.1$, $\gamma=0$, $K=3$, $\tau=3\pi$, $\omega_1=0.997\,57$, $\omega_2=0.990\,98$, $\omega_3=1.015\,18$, and $\omega_4=0.994\,96$.

To illustrate this further and demonstrate the robustness of our stability results for slightly nonidentical oscillators, we choose a set of control parameters $K=3$ and $\tau=3\pi$, denoted by the black cross in Fig. 3(a), for which multistability of all four possible synchronization states is found for the coupling phase $\beta=0$. Figures 3(b)–3(e) show time series from numerical simulations of four Stuart-Landau oscillators in a unidirectional ring configuration with slightly different frequencies ω. For each choice of β in panel (b)–(e) the solutions Ω_m were obtained by solving Eqs. (2) such that the solution of Ω_m closest to unity was chosen. The differences of the phases φ_i ($i=2,3,4$) relative to the first oscillator phase φ_1 are plotted. After transients (note that the transient oscillations are not resolved on the time scale chosen), the oscillators behave exactly as predicted by our theory, i.e., they lock into in-phase synchronization for $\beta=\Omega_0\tau$ (b), into a splay state for $\beta=\Omega_1\tau-\pi/2$ (c), into a two-cluster state for $\beta=\Omega_2\tau-\pi$, where $\varphi_1=\varphi_3$ and $\varphi_2=\varphi_4$ (d), and again into a splay state, albeit with inverted ordering of the phases, for $\beta=\Omega_3\tau-3\pi/2$ (e).

Finally, for the subcritical Hopf normal form, it can be shown that the periodic orbit, which is unstable in the uncoupled case, can be stabilized in-phase synchronously by,

e.g., bidirectional ring, star, or all-to-all coupling without self-feedback. In these cases, both the synchronization manifold and the transversal modes are stable. There, Floquet exponents Λ satisfy again Eq. (7) with $\nu_0=\mu$. For proper coupling phases β, we find a finite interval of feedback gain K for which the real parts of all Floquet exponents are negative. Note that the in-phase synchronization manifold coincides with a single oscillator with delayed self-feedback as considered in Ref. [17] to refute the alleged odd number limitation.

For all-to-all coupling the adjacency matrix is given by $a_{i,i}=0$ and $a_{i,j}=1$ for $i\neq j$ and $i,j=1,\ldots,N$, while for star coupling all $a_{i,j}=0$, except $a_{1,i}=1$ and $a_{i,1}=N-1$ for $i=2,\ldots,N$. Figure 4 shows Re Λ in the subcritical case as a function of coupling strength μK for all-to-all and star coupling. The solid (blue) lines correspond to Re Λ inside the synchronization manifold ($\nu_0=\mu=N-1$ for both coupling configurations). For all-to-all coupling the transversal eigenvalues of $\mathbf{A}$ are given by $\nu_k=-1$ for $k=1,\ldots,N-1$ and the corresponding largest Re Λ are denoted by the dashed (red) lines in Fig. 4 for different N. For star coupling, the transversal eigenvalues of $\mathbf{A}$ are $\nu_k=0$ for $k=1,\ldots,N-2$ and $\nu_{N-1}=-(N-1)$, and the corresponding largest Re Λ are marked schematically. We stress that for both all-to-all and star coupling there exists an interval of feedback strength K in which all Re $\Lambda<0$. Thus, time delayed coupling results in stabilization and in-phase synchronization.

In conclusion, we have shown that by tuning the coupling phase in delay-coupled networks one can easily control the stability of synchronous periodic states, and we have specified analytic conditions. In general networks in-phase synchronization or desynchronization can be chosen, and in unidirectional rings either in-phase cluster or splay states can be selected. The coupling phase is a parameter which is readily accessible, e.g., in optical experiments [1]. Our results are robust even for slightly nonidentical elements of the network.

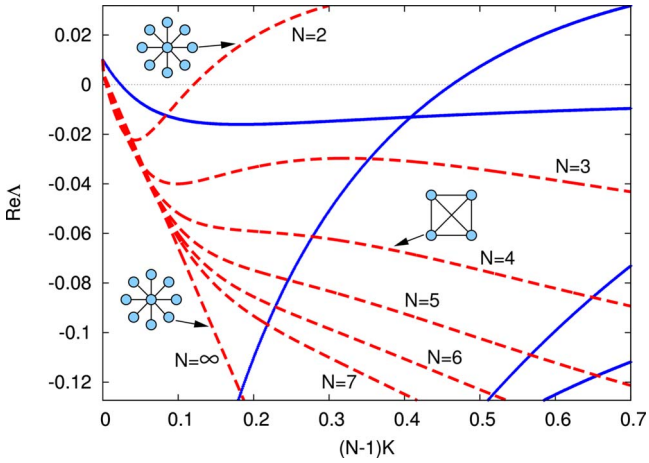

FIG. 4. (Color online) Real part of the Floquet exponents Λ in the subcritical case vs reduced coupling strength $(N-1)K$ in the all-to-all and star coupling configurations for different N. The solid (blue) lines denotes Re Λ inside the synchronization manifold for both all-to-all and star coupling. The dashed (red) lines show the largest transversal Re Λ for different N and all-to-all coupling. Floquet exponents for star coupling are independent of N and marked schematically. Parameters (as in [17]): $\lambda=-0.005$, $\omega=1$, $\gamma=-10$, $\tau=2\pi/(1-\gamma\lambda)$, and $\beta=\pi/4$.

C.-U. C. acknowledges support from Alexander von Humboldt Foundation. This work was also supported by DFG in the framework of Sfb 555. We thank A. Amann for valuable discussions.

[1] *Handbook of Chaos Control*, 2nd ed., edited by E. Schöll and H. G. Schuster (Wiley-VCH, Weinheim, 2008).
[2] D. J. Watts and S. H. Strogatz, Nature **393**, 440 (1998); R. Albert and A.-L. Barabási, Rev. Mod. Phys. **74**, 47 (2002); M. E. J. Newman, SIAM Rev. **45**, 167 (2003); A.-L. Barabási and E. Bonabeau, Sci. Am. **288**, 50 (2003); S. Boccaletti *et al.*, Phys. Rep. **424**, 175 (2006).
[3] L. M. Pecora and T. L. Carroll, Phys. Rev. Lett. **80**, 2109 (1998).
[4] M. Dhamala, V. K. Jirsa, and M. Ding, Phys. Rev. Lett. **92**, 074104 (2004); V. K. Jirsa, Cognit. Neurodynamics **2**, 29 (2008).
[5] W. Kinzel, A. Englert, G. Reents, M. Zigzag, and I. Kanter, Phys. Rev. E **79**, 056207 (2009).
[6] I. Fischer *et al.*, Phys. Rev. Lett. **97**, 123902 (2006).
[7] R. Vicente *et al.*, Proc. Natl. Acad. Sci. U.S.A. **105**, 17157 (2008).
[8] V. Flunkert, O. D'Huys, J. Danckaert, I. Fischer, and E. Schöll, Phys. Rev. E **79**, 065201(R) (2009).
[9] D. V. Ramana Reddy, A. Sen, and G. L. Johnston, Phys. Rev. Lett. **85**, 3381 (2000).
[10] M. Gassel *et al.*, Fluct. Noise Lett. **7**, L225 (2007).
[11] M. Bonnin *et al.*, Int. J. Bifurcation Chaos Appl. Sci. Eng. **17**, 4033 (2007).
[12] E. Schöll *et al.*, Philos. Trans. R. Soc. London, Ser. A **367**, 1079 (2009).
[13] M. G. Earl and S. H. Strogatz, Phys. Rev. E **67**, 036204 (2003).
[14] O. D'Huys *et al.*, Chaos **18**, 037116 (2008).
[15] G. C. Sethia, A. Sen, and F. M. Atay, Phys. Rev. Lett. **100**, 144102 (2008).
[16] K. Pyragas, Phys. Lett. A **170**, 421 (1992).
[17] B. Fiedler, V. Flunkert, M. Georgi, P. Hövel, and E. Schöll, Phys. Rev. Lett. **98**, 114101 (2007).
[18] K. Pyragas and T. Pyragiene, Phys. Rev. E **78**, 046217 (2008).
[19] R. Zillmer, R. Livi, A. Politi, and A. Torcini, Phys. Rev. E **76**, 046102 (2007).
[20] Note that d_c clusters can also exist in more general networks, e.g., with circulant adjacency matrix.